

REPORT DOCUMENTATION PAGE				Form Approved OMB No. 0704-0188	
<p>Public reporting burden for this collection of information is estimated to average 1 hour per response, including the time for reviewing instructions, searching existing data sources, gathering and maintaining the data needed, and completing and reviewing this collection of information. Send comments regarding this burden estimate or any other aspect of this collection of information, including suggestions for reducing this burden to Department of Defense, Washington Headquarters Services, Directorate for Information Operations and Reports (0704-0188), 1215 Jefferson Davis Highway, Suite 1204, Arlington, VA 22202-4302. Respondents should be aware that notwithstanding any other provision of law, no person shall be subject to any penalty for failing to comply with a collection of information if it does not display a currently valid OMB control number. PLEASE DO NOT RETURN YOUR FORM TO THE ABOVE ADDRESS.</p>					
1. REPORT DATE (DD-MM-YYYY) May 2012		2. REPORT TYPE Technical Paper		3. DATES COVERED (From - To) May 2012-June 2012	
4. TITLE AND SUBTITLE Trajectory and Mixing Scaling Laws for Confined and Unconfined Transverse Jets				5a. CONTRACT NUMBER In-House	
				5b. GRANT NUMBER	
				5c. PROGRAM ELEMENT NUMBER	
6. AUTHOR(S) D. Forliti				5d. PROJECT NUMBER	
				5e. TASK NUMBER	
				5f. WORK UNIT NUMBER 33SP0795	
7. PERFORMING ORGANIZATION NAME(S) AND ADDRESS(ES) Air Force Research Laboratory (AFMC) AFRL/RQRE 4 Draco Drive. Edwards AFB CA 93524-7160				8. PERFORMING ORGANIZATION REPORT NO.	
9. SPONSORING / MONITORING AGENCY NAME(S) AND ADDRESS(ES) Air Force Research Laboratory (AFMC) AFRL/RQR 5 Pollux Drive Edwards AFB CA 93524-7048				10. SPONSOR/MONITOR'S ACRONYM(S)	
				11. SPONSOR/MONITOR'S REPORT NUMBER(S) AFRL-RZ-ED-TP-2012-203	
12. DISTRIBUTION / AVAILABILITY STATEMENT Distribution A: Approved for Public Release; Distribution Unlimited. PA#12437					
13. SUPPLEMENTARY NOTES Conference paper for the AIAA Fluid Dynamics Conference, New Orleans, LA, 25-28 June 2012.					
14. ABSTRACT Transverse jets play an important role in many propulsion-related applications including gas turbine burner dilution, exhaust from V/STOL aircraft, and fluidic thrust vectoring. Although this flow has received extensive research attention over several decades, a lack of universality exists regarding scaling laws available in literature. Using data from existing literature, a foundational scaling law framework has been proposed for the jet trajectory and mixture uniformity. A newly derived parameter demonstrates an improved collapse of trajectory data in literature. This parameter was derived using theoretical arguments that both entrainment and aerodynamic drag should be considered as relevant mechanisms of momentum transport between the jet and cross flow. An experimental study was conducted and the results indicate the utility of the new scaling law parameter for defining flow regimes and correlating mixing performance. Future work will extend this scaling law framework for multiple transverse jet configurations.					
15. SUBJECT TERMS					
16. SECURITY CLASSIFICATION OF:			17. LIMITATION OF ABSTRACT	18. NUMBER OF PAGES	19a. NAME OF RESPONSIBLE PERSON
a. REPORT	b. ABSTRACT	c. THIS PAGE			Nils Sedano
Unclassified	Unclassified	Unclassified	SAR	14	19b. TELEPHONE NO (include area code) 661-275-5972

Trajectory and Mixing Scaling Laws for Confined and Unconfined Transverse Jets

David J. Forliti¹

Jackson and Tull/AFRL-RZSE, Edwards AFB, CA, 93524

Transverse jets play an important role in many propulsion-related applications including gas turbine burner dilution, exhaust from V/STOL aircraft, and fluidic thrust vectoring. Although this flow has received extensive research attention over several decades, a lack of universality exists regarding scaling laws available in literature. Using data from existing literature, a foundational scaling law framework has been proposed for the jet trajectory and mixture uniformity. A newly derived parameter demonstrates an improved collapse of trajectory data in literature. This parameter was derived using theoretical arguments that both entrainment and aerodynamic drag should be considered as relevant mechanisms of momentum transport between the jet and cross flow. An experimental study was conducted and the results indicate the utility of the new scaling law parameter for defining flow regimes and correlating mixing performance. Future work will extend this scaling law framework for multiple transverse jet configurations.

Nomenclature

B	= new trajectory scaling parameter
C_D	= drag coefficient
C	= Holdeman parameter
C_I	= constant
c_{ej}	= entrainment coefficient
D	= diameter
h	= height of crossflow control volume
H	= height of channel
J	= momentum flux ratio
l_o	= momentum-based cross flow length scale
\dot{m}	= mass flow rate
n	= number of jets
Q	= volume flow rate
r	= velocity ratio
R	= main pipe radius
$R_{1/2}$	= half-area radius
S	= jet spacing
U	= bulk velocity
U_z	= unmixedness
x	= streamwise coordinate
y	= cross stream coordinate
β	= momentum ratio
ρ	= fluid density
o	= subscript for main flow
j	= subscript for jet flow
Z	= mixture fraction
σ	= standard deviation

¹ Research Scientist, Jackson and Tull, AFRL/RZSE, 4 Draco Drive, Bldg. 8351, rm. 124A, Senior Member.

I. Introduction

TRANSVERSE jets have received extensive research attention during the past several decades, due to their relevance in a number of applications including chemical dispersion in the environment, film cooling, fluidic thrust vectoring, dilution in gas turbine combustion chambers, and V/STOL aircraft, to name a few. Much of the research to date has focused on the single unconfined transverse jet as a canonical three-dimensional flow for building the knowledge base and tools that can be employed for the design of specific applications. Review articles on the transverse jet have been provided by Margason¹ and Karagozian².

A schematic of the flow field of a single transverse jet, adopted from Fric and Roshko³, is shown in Fig. 1. A variety of flow structures have been identified, and the mechanisms associated with the formation of these structures have been the subject of many studies. The globally dominant feature of the transverse jet is the counter-rotating vortex pair (CVP). The mechanism responsible for the formation of the CVP has been a central research topic for many studies.^{e.g. 4-9} The general view from this body of work is that the vorticity present in the CVP forms through a reorientation and alignment of the azimuthal vorticity of the jet, notwithstanding that the details of this mechanism are not fully understood and appears to be very complex. The instability and scaling characteristics of the near-field shear layer has been extensively explored by Karagozian and coworkers.^{10, 11}

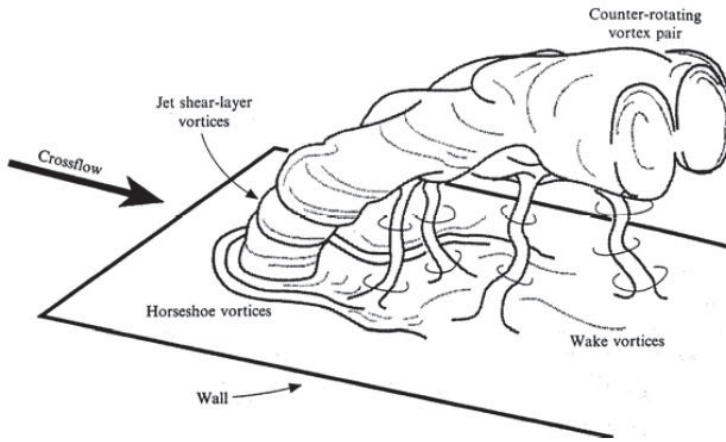


Figure 1. Structure of the transverse jet (adopted from Fric and Roshko [3]).

It is clear that one of the main themes in transverse jet literature is the development of scaling laws that can be used to predict the behavior of the jet, particularly the trajectory. These scaling law development efforts focused on incompressible flow with equal density for the jet and crossflow. Keffer and Baines¹² first proposed trajectory scaling using a length scale of $r^2 D_j$, where r is the ratio of the jet velocity U_j to the crossflow velocity U_o , and D_j is the diameter of the jet. Pratte and Baines¹³ followed up on the work of Keffer and Baines, leading to the emergence of a

proposed $r D_j$ characteristic length scale for normalizing the trajectory. Broadwell and Briedenthal⁴ derived the $r D_j$ scaling law form through arguments that a length scale in the crossflow, referred to here as l_o , can be defined as

$$l_o = \frac{U_j D_j}{U_o} \quad (1)$$

which essentially matches the momentum of the crossflow passing through an area with a diameter of l_o to the momentum of the jet. Hasselbrink and Mungal¹⁴ also arrive at an $r D_j$ scaling law through an entrainment-based argument. The scaling law model for jet entrainment, based on work done by Ricou and Spalding¹⁵, has the form

$$\frac{1}{\dot{m}_j} \frac{d\dot{m}}{dx} = c_{ej} \left(\frac{\rho_o}{\rho_j} \right)^{1/2} \frac{1}{D_j} \quad (2)$$

where \dot{m} is the local mass flow rate in the jet, x is the streamwise coordinate, c_{ej} is the entrainment rate coefficient, ρ is the fluid density, and the subscripts o and j represent the crossflow and jet, respectively. The nominal value for c_{ej} for a fully-developed round free jet is 0.32.

Although most of the transverse jet studies have considered single unconfined jets, effort has also been placed on understanding confined transverse jet mixing, primarily motivated by gas turbine combustion chamber design.

Performance demands for turbine-based propulsion systems lead to the maximization of turbine inlet pressures. To avoid damage and wear on the high-pressure turbine, the combustor should deliver a highly uniform hot gas mixture to the turbine, requiring efficient mixing of dilution air in the combustor. Motivated by this design problem, Holdeman and coworkers have over a period of several decades conducted research on a very wide range of configurations and flow conditions; a review of much of this work is provided by Holdeman¹⁶⁻¹⁸. Review of the vast experimental and computational data obtained by Holdeman and coworkers¹⁹ has lead to an empirical correlation,

$$C = \frac{S}{H} \sqrt{J} \quad (3)$$

where C is a constant that indicates the level of uniformity at a defined distance downstream, S is the spanwise spacing between neighboring jets, H is the (two-dimensional) channel height, and J is the momentum flux ratio, defined as

$$J = \frac{\rho_j U_j^2}{\rho_o U_o^2} \quad (4)$$

Holdeman established that for optimum mixing, defined in terms of the spatial distribution of the mean scalar (e.g. temperature) field, C should have a nominal value of 2.5. Values of C of 1.25 and below represent poor mixing due too underpenetration, and values of 5 and above represent overpenetration. It is interesting to note that the Holdeman parameter does not depend on the jet diameter. Deviations from this scaling law have been observed when the mass flow ratio of injected to main flow becomes large, or when opposing walls contain spanwise staggered jets.²⁰ Nonetheless, the utility of the Holdeman parameter as a design guide has been demonstrated under gas turbine relevant conditions.^{21, 22} The Holdeman parameter has been successfully extended to circular main-flow geometries, through defining the jet spacing distance S at the R/2 radius that is the radius that divides the round duct into two equal areas

$$R_{1/2} = R / \sqrt{2} \quad (5)$$

where R is the duct radius. In terms of the number of jets n distributed on the circumference of the duct,

$$S = \frac{2\pi R_{1/2}}{n} \quad (6)$$

It should be mentioned that most of the gas turbine related research on multiple mixing jets in a round duct include eight to twenty jets. Additionally, the Holdeman scaling law is based on evaluating mixedness properties in the near field of the injection, nominally one main duct diameter. It is uncertain if the Holdeman rule applies for downstream locations.

A related configuration that has received extensive attention from the chemical processing research community is the tee mixer, consisting of a single transverse jet issuing into a round pipe.²³⁻²⁷ Efforts to construct mixing performance scaling laws have been the primary subject of interest with regards to the tee mixer. O'Leary and Forney²⁸ determined the optimum velocity ratio for a variety of diameter ratios, defining the optimum mixing condition to be associated with flow conditions that place the asymptote of the jet trajectory along the centerline of the pipe. A subsequent study by Sroka and Forney²⁹ involved a global mixing quality scaling law in terms of the momentum ratio β defined as

$$\beta = \frac{\rho_j U_j^2 D_j^2}{\rho_o U_o^2 D_o^2} \quad (7)$$

The data indicated that mixing in the downstream region benefits from a strong nearfield impaction of the jet on the wall that occurs at momentum ratios above unity. This mixing mechanism is stated as being dominated by the impingement process and not jet entrainment. It is interesting to note that research has shown that chemical reaction

yield, particularly for competing reactions, have shown an optimum velocity ratio exists for product formation, with detrimental effects associated with strong jet impaction.³⁰ This observation highlights the difference in defining mixing in terms of macroscale bulk mixing based on mean scalar distributions, and microscale mixing associated with instantaneous mixture composition required for chemical reactions. A more recent study by Forney, Nafia, and Vo indicated that prior to enhanced mixing associated with strong jet impaction on the wall, a local optimum state is associated with moderate impaction on the wall.³¹ Unlike the Holdeman scaling law for multiple confined transverse jets, the mixing properties for the tee mixer is strongly dependent on the jet diameter.

II. Revisiting Single Unconfined Transverse Jet Trajectory Scaling

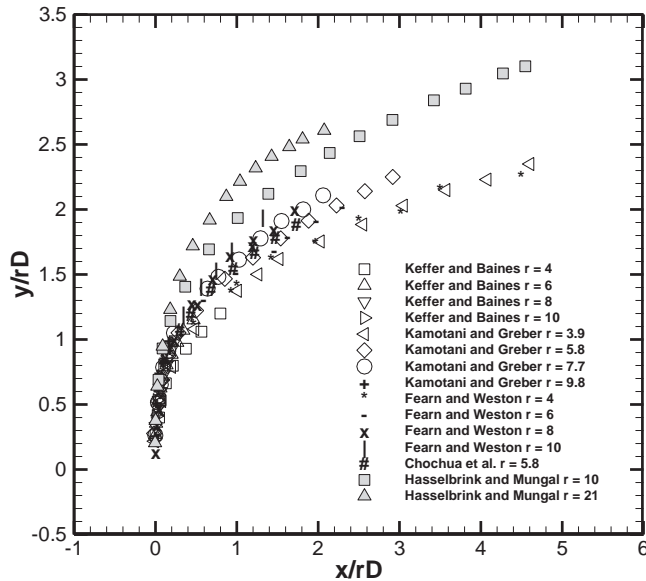


Figure 2. rD_j scaling of jet trajectory data from literature.

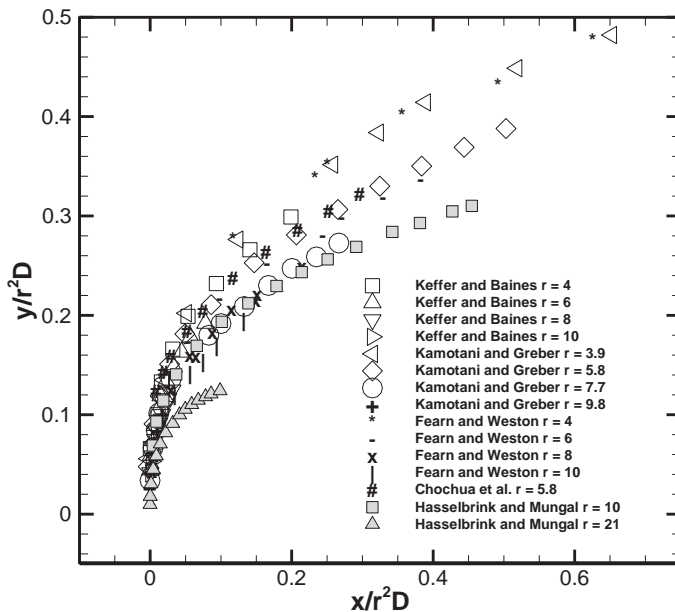


Figure 3. r^2D_j scaling of jet trajectory data from literature.

As mentioned previously, scaling of the transverse jet trajectory has been of interest to the research community. The two primary scaling laws developed in literature involve normalizing the trajectory coordinates by rD_j or r^2D_j . Figure 2 shows the trajectories from literature normalized using rD_j . Data in Fig. 2 is limited to cases that measure the trajectory based on velocity measurements, have a moderate to high jet Reynolds number (larger than approximately 2000), and velocity ratios near or above 4. Velocity ratios below 4 are generally weak jets where the jet structure is highly disturbed by the interaction with the crossflow and may have more or less wake like characteristics. Note that the rD_j scaling can be derived through arguments of entrainment-dominated momentum transfer to the jet. All data except the Hasselbrink and Mungal data involved a top-hat velocity profile for the jet as generated with a large area-ratio nozzle; the Hasselbrink and Mungal data is for a fully-developed pipe flow for the jet.

Figure 3 shows the r^2D_j scaling law using data from literature. The r^2D_j scaling law form was originally proposed through the argument that the drag on the jet column is the dominant mechanism for momentum transfer between the crossflow and the jet. It is clear from Figs. 2 and 3 that the rD_j and r^2D_j scaling laws do not provide a strong correlation of jet trajectory data across different velocity ratios and experimental facilities. There have been attempts in recent years to modify the scaling laws to account for the jet exit velocity profile and the crossflow boundary layer.^{32, 33}

As the two primary scaling law approaches have employed either entrainment or drag mechanisms of momentum interaction between the jet and crossflow, a new scaling law framework is

desired that incorporates both of these mechanisms in a simplified formulation. For jets with velocity ratios above 4, it is likely that the entrainment in the jet nearfield is likely very similar to a free jet, suggesting that the entrainment model of Ricou and Spalding may be used. As the jet issues into the crossflow, a drag force is present on the jet column. This force can be modeled using the drag coefficient. A model of a liquid transverse jet interacting with a gas crossflow has been developed by Mashayek et al.³⁴ A nominal drag coefficient on the jet column of 1.7 was determined from this study. The value is significantly larger than the drag coefficient for a round cylinder in crossflow due to the fact that the jet distorts into an elliptic cross section with enhanced blockage to the crossflow. A parameter can be developed by incorporating these two momentum transfer mechanisms. A new parameter B can be defined as the ratio of initial jet momentum to the momentum transported to the jet in a characteristic streamwise distance (relative to the jet flow direction) is

$$B = \frac{J}{\frac{2C_D}{\pi} + c_{ej} J^{1/2}} \quad (8)$$

where C_D is the drag coefficient. It is interesting to note that B is proportional to r^2 when the entrainment mechanism is neglected, while it is proportional to r when the drag mechanism is neglected. The length scale BD_j represents the streamwise distance where the magnitude of the new momentum added through entrainment and drag is equal to the original jet momentum.

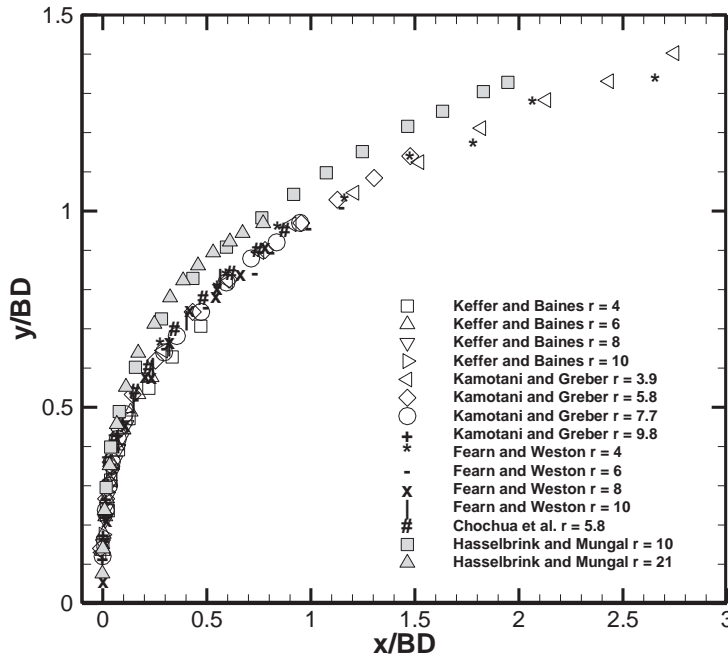


Figure 4. BD_j scaling of jet trajectory data from literature.

the data, particularly in the far field, is surprising considering that the drag coefficient is likely only accurate in the near field of the jet.

It should be added that there is data in literature that has not been included in Figs. 2-4. e.g. 13, 33, 36-38 These cases were not considered due to low jet Reynolds number, an excessively thick crossflow boundary layer, or trajectories based on scalar field measurements. Reynolds number and boundary layer thickness directly influence the momentum transport mechanisms.

The BD_j scaling law represents a good starting point for correlating transverse jets. For the target application of preburners for liquid rocket engines, issues of confinement, very large density ratio, and super/transcritical effects complicate the utility of the BD_j scaling law. Research is currently being planned to address these effects.

Figure 4 shows the jet trajectory scaled using the BD_j scaling. It is seen that the new parameter is able to provide a strong correlation across the range of cited literature data. The Hasselbrink and Mungal data has a slightly deeper penetration than the jets with a top-hat exit profile. It has been established that the entrainment rate in the near field of jets issuing from fully-developed pipe flow is reduced and gradually approaches the Ricou and Spalding rate with increasing downstream distance.³⁵ Such a reduction in entrainment will reduce momentum transport to the jet, resulting in the enhanced penetration. The Hasselbrink and Mungal trajectories eventually approach a parallel curve to the other data as the entrainment rate evolves along the jet trajectory. The collapse of

III. Optimum Mixing Scaling Laws for Confined Transverse Jets

For designers of applications involving confined mixing devices that employ transverse injection, scaling laws for optimum mixing are very useful for guiding the design evolution. The work of Forney, Nafia, and Vo³¹ resulted in an optimized jet mixing scaling law for the tee mixer having the form

$$\frac{D_j}{D_o} = C_1 \left(\frac{Q_j}{Q_o} \right)^{2/3}, \quad (9)$$

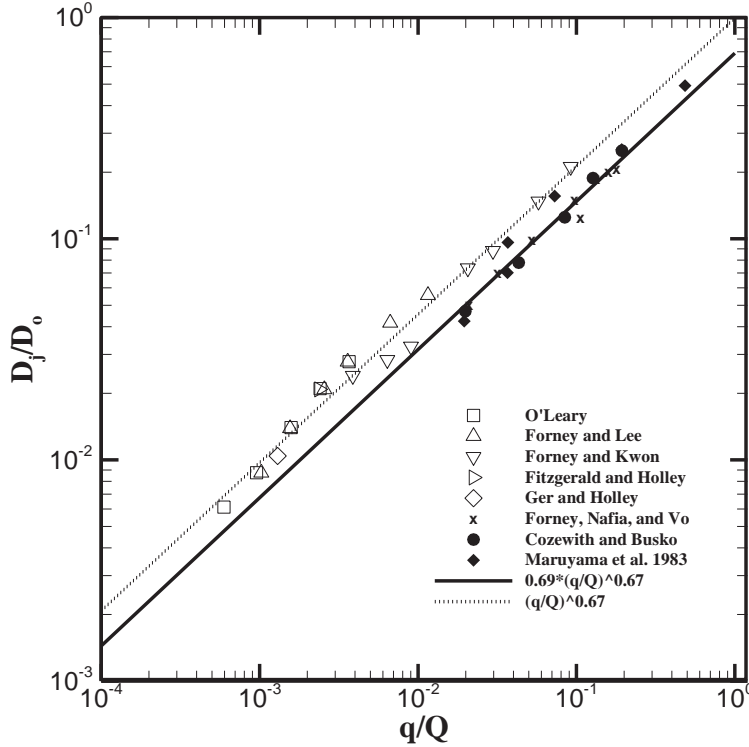


Figure 5. Optimized mixing condition scaling law for tee mixers.

pipe, whereas the filled symbols represent optimization based on chemical reaction. The scaling law form shown in Eq. 9 with a coefficient C_1 of unity matches the jet-centered data.

Due to the fact that the volumetric flow ratio can be replaced with the product of the velocity ratio and the diameter ratio squared, Eq. 9 can be restated as

$$r^2 \left(\frac{D_j}{D_o} \right) = \frac{1}{C_1^3}, \quad (10)$$

which shares the general form of $r^2 D_j$ proposed by Keffer and Baines¹² for unconfined single transverse jets.

One of the objectives of the current research effort is to establish physics-based scaling laws for confined mixing devices that employ transverse jets. Figure 6 illustrates three possible candidate scaling formulations for the tee mixer. Figure 6(a) is a schematic of a circular region with a diameter of l_o used to match momentum of the main flow and jet. This is a natural extension of the unconfined arguments that lead to the establishment of cross flow length scale given in Eq. 1. Figure 6(b) illustrates a modified crossflow region that is rectangular in shape, having one side equal to the jet diameter D_j and a height h that would be defined to match crossflow momentum of the jet. The proposed regions in Figs. 6(a) and (b) have the same area, but differ only in how the crossflow interaction area is defined. Figure 6(c) illustrates that the unconfined trajectory length scale $B D_j$ is the relevant governing scale.

where Q is the volumetric flow rate (this study was based on incompressible flow with equal density for the jet and main flow), and C_1 is an empirical constant equal to 0.69. This is apparently the mixing optimum condition prior to strong impaction where jet entrainment still plays an important role. Figure 5 shows data from literature on the optimized tee mixer in the jet mixing regime. Using a semi-empirical jet trajectory scaling model, Forney and coworkers derive the $2/3$ power through fixing the trajectory such that it would impact the opposite wall at a streamwise position that is one-half pipe diameter downstream of the injection location (termed moderate impaction). This derived relation is limited to D_j/D_o values above 0.08, although data from other studies appear to follow this trend to diameter ratios down to 0.02 as seen in Fig. 5. The hollow symbols represent conditions that place the jet at the center of the

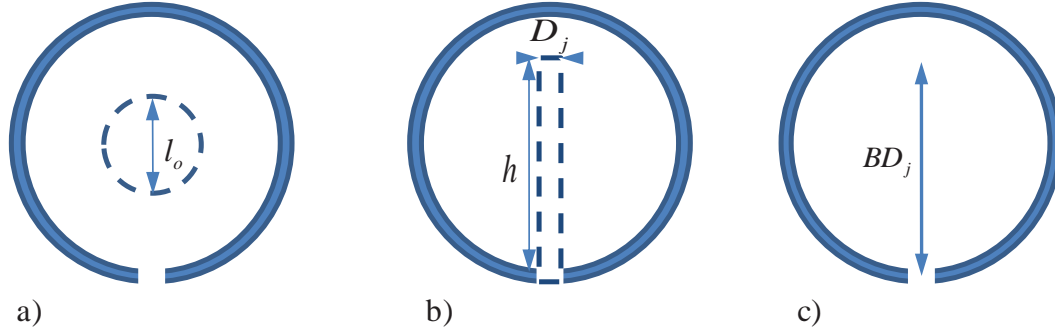


Figure 6. Domain of crossflow interaction assuming a) circular and b) rectangular areas and c) BD_j penetration scaling.

As mentioned earlier in the discussion of literature of the tee mixer research, it is anticipated that the condition associated with optimum mixing implies that the jet penetrates far into the pipe, and in fact experiences moderate impaction on the opposite side of the pipe. At this condition, it can be argued that the various scales in Fig. 6 should be proportional to the pipe diameter D_o . For the configuration shown in Fig. 6(a), arguing that l_o is proportional to the pipe diameter results in a constant momentum ratio β as defined in Eq. 7.

Matching the momentum of the main flow passing through the rectangular section shown in Fig. 6(b) with the momentum of the jet yields

$$D_j D_o U_o^2 = D_j^2 U_j^2, \quad (11)$$

an expression that can be further simplified to

$$r^2 \frac{D_j}{D_o} = 1. \quad (12)$$

Equation 12 is shown in Fig. 5 as the dotted curve, and it is seen that pipe-centered optimization data agrees well with this equation. As stated earlier, this form was derived by Forney and coworkers through more elaborate modeling of the trajectory employing semi-empirical models for entrainment. It is apparent that the improved performance of the correlation with C_1 equal to 0.69, as shown in Fig. 5, suggests that the jet momentum should be proportional, but higher, than the main flow momentum.

The new BD_j unconfined transverse jet scaling law can be employed for the Tee mixer as well. It is conjectured that BD_j should be proportional to the main flow pipe diameter D_o . Setting these two length scales equal suggests that

$$B \frac{D_j}{D_o} = 1. \quad (13)$$

Figure 7 shows the optimized mixing configuration data from Fig. 5 recast in terms of velocity ratio as a function of diameter ratio. The centered jet data is not included because these cases are not optimum in mixing performance. The momentum ratio of unity has the correct trend but strongly overpredicts the optimum velocity ratio for smaller diameter ratios. Consideration of different constant values of the momentum ratio could improve the correlation at low diameter ratio at the cost of accuracy at high diameter ratio. The scaling associated with Eq. 10 with a constant of 0.69 appears to correlate relatively well with the experimental data points. The BD_j scaling correlation has the strongest correlation to the measured values. The correlation coefficient of the BD_j and Eq. 10 scaling laws are 0.97 and 0.90, respectively.

One of the primary effects of the confinement is that the entrainment into the transverse jet may be constrained by the finite main flow. The transverse jet entrains crossflow fluid as the jet follows the trajectory across the main duct. The Ricou and Spalding model can be used to estimate the total mass flow rate entrained into the jet as the jet travels across the pipe,

$$\frac{\dot{m}_{entrained}}{\dot{m}_o} = 0.32 \frac{D_j}{D_o} r \quad (14)$$

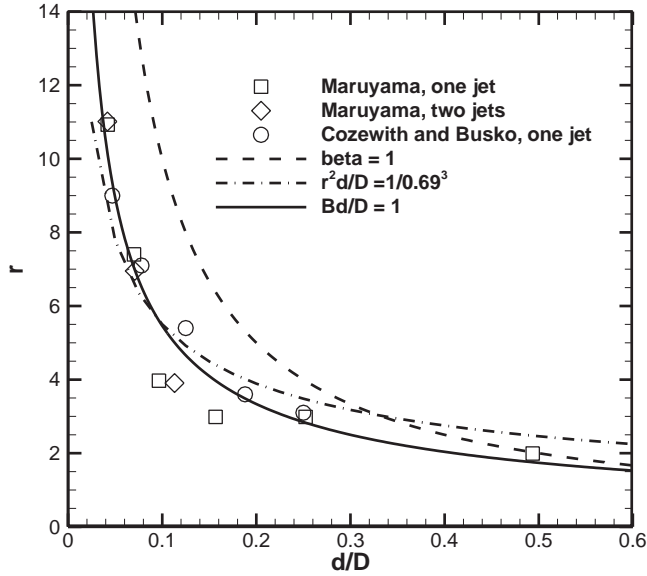


Figure 7. Optimum correlations for tee mixers.

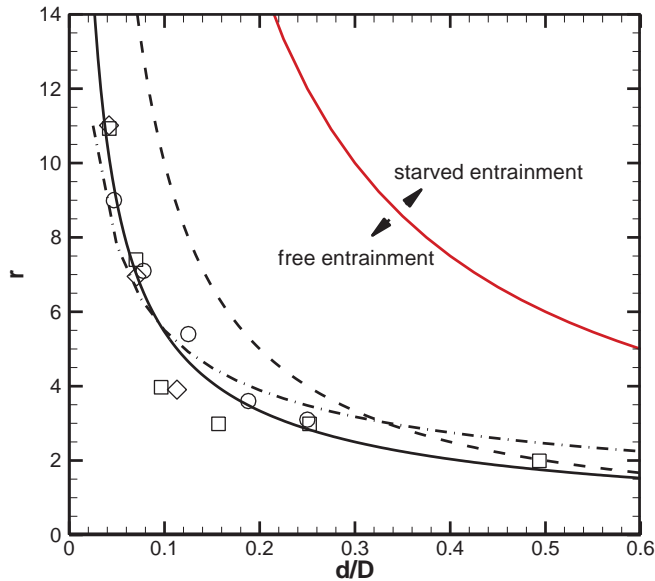


Figure 8. Entrainment limit boundary on single and two jet configurations.

the momentum through this region to the jet momentum yields

$$r^2 \frac{D_j}{R_o} = 1 \quad (15)$$

This ratio cannot be larger than unity. The boundary defined by this condition is shown in Fig. 8 including the data originally shown in Fig. 7. The figure demonstrates that the data is far from this boundary, and the jet is expected to entrain without excessive confinement effects. As will be shown next, this effect of confinement will complicate the scaling of mixing for configurations will many (more than eight) transverse jets.

Figure 9 shows the entrainment limit boundary for three relative mass flow rates as a function of velocity ratio and number of jets. Also indicated on the plot is the optimum velocity ratio as a function of the number of jets based on the empirical correlation of Holdeman. The number of jets range from eight to sixteen, a typical range applicable for gas turbine burner configurations^{e.g. 22}. The general trend is that the jets experience entrainment starvation when the number of jets or the mass flow ratio is increased. The study by Leong, Samuelsen, and Holdeman²² was for a mass flow ratio of 2.5, suggesting that this particular study experienced constrained jet entrainment. The results of Fig. 9 indicate that a more sophisticated framework will be required to parameterize the entrainment effect for situations with several transverse jets. Additionally, the confinement effect will modulate the drag on the jet. The confinement forces the crossflow to accelerate due to the blockage provided by the jet, a mechanism that expected to increase drag and reduce jet penetration. Characterizing the effects of confinement on the entrainment and drag behavior will be investigated in future research.

As a final note, the form of the Holdeman parameter given in Eq. 3 can be derived using simple arguments that are supported by evidence in the literature. Using an interaction region as shown in Fig. 6(b) but extending only to the centerline due to multiple jets, matching

Using the observation that the dimensions of the jet, in particular in the cross section scale with rD_j^{37} , and requiring that this length scale is proportional to the jet spacing,

$$rD_j \propto S, \quad (16)$$

leads to

$$r \frac{S}{R_o} \propto 1. \quad (17)$$

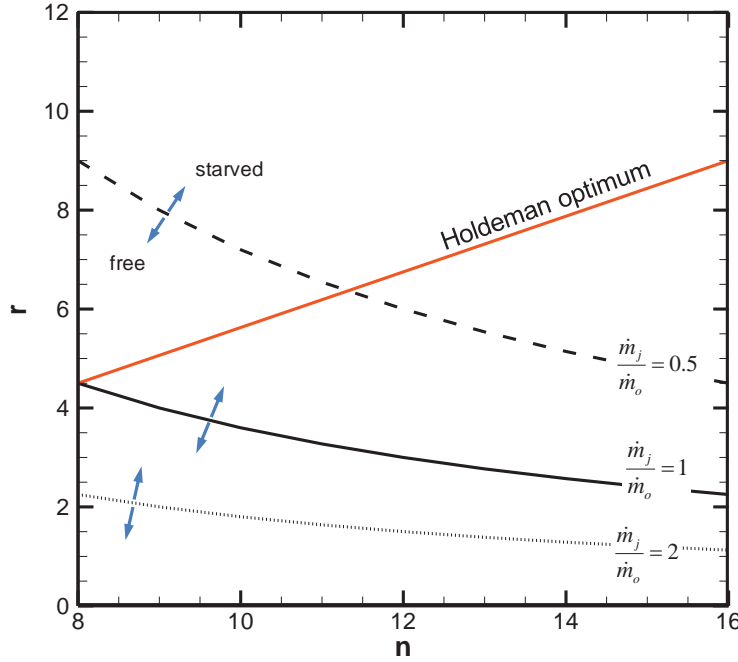


Figure 9. Entrainment limit boundaries and the Holdeman scaling law.

becomes comparable to the pipe radius. For large jet spacing S , the jets will begin to interact with each other as they approach the scale of the pipe radius, which is smaller than the spacing. Large jet spacing is a design regime that must be explored in future research.

The existing scaling laws for tee mixers and gas turbine combustors (i.e. Holdeman and related efforts) do not span the full range in terms of the number of jets. The tee mixer scaling law, that also appears to be valid for two jets, depends strongly on the jet size and is associated with an impingement regime. The Holdeman correlation developed for the gas turbine combustor application is primarily validated for eight to twenty jets, does not depend on the jet size, and is associated with a non-impinging regime. It is possible that evaluation of the gas turbine configurations at further downstream distances will lead to impinging regimes being optimum with different scaling law forms. Finally, the literature gap in the number of jets, namely two to eight, must be addressed, in particular due to the fact that current rocket preburner designs fall in this range.

IV. Experimental Apparatus

Holdeman finds that the term on the right side of Eq. 17 is nominally equal to 2.5 for optimum mixing. The requirement of Eq. 16 ensures that the developed structures of neighboring transverse jets begin to merge together to facilitate good mixing. With rD_j being too small, the jets will not merge quickly, requiring further streamwise extent for uniform mixing to develop. Having too large of an rD_j value will lead to inhibition of the counter-rotating vortex pair formation mechanism, which is a driver for enhanced mixing in the transverse jet. This framework will be revised once additional information on drag and entrainment is available. Additionally, it appears that arguing that rD_j scales with S will likely breakdown when the number of jets is reduced, due to the fact that the jet spacing S

An experiment underway at the Air Force Research Laboratory at Edwards Air Force Base is motivated to investigate confined mixing using multiple transverse jets. The purpose of the experiment is to establish scaling laws in the gap region between single confined transverse jets and the higher jet number cases (8-20 jets)²² that have

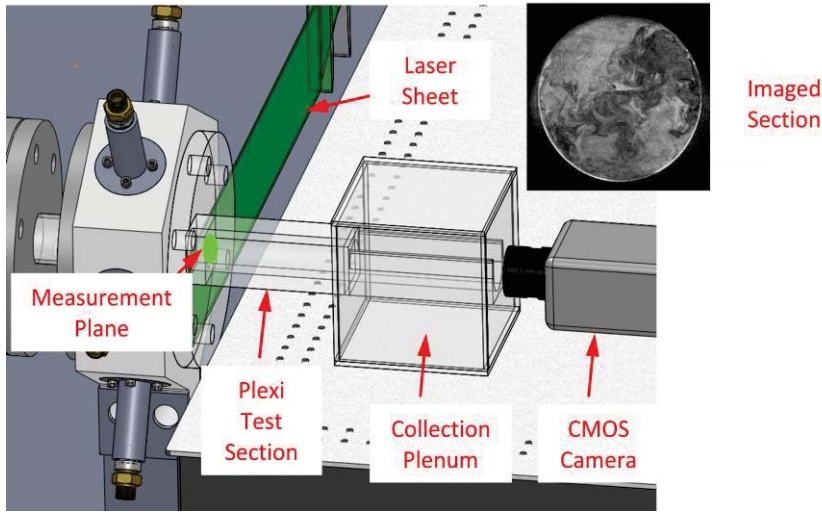


Figure 10: Schematic of the confined jet mixing experimental setup.

The mixing was investigated through the employment of planar laser induced fluorescence (PLIF). Sodium fluorescein was added to the water supply for the jets, which absorbs and emits in a band centered on 490 and 519 nm, respectively.³⁹ The fluorescence is induced using the 488 nm line of a 225 mW argon-ion laser (National Laser model 800AL). The 488 nm line is isolated from the multiline laser output using an Edmund Optics dichroic mirror. A Phantom V7.1 CMOS camera is used to capture PLIF images; a sample short exposure time image is shown in Fig. 10. A Thorlabs long pass optical filter is placed between the camera and the light sheet to remove the 488 nm from the fluorescence signal. Calibration images were collected for uniform mixtures at different concentration levels. The camera and the fluorescence were independently verified as being nominally linear in the range used for the experiments. The fluorescein concentration in the test section was found to be below approximately 3×10^{-7} mol/L, a level that corresponds

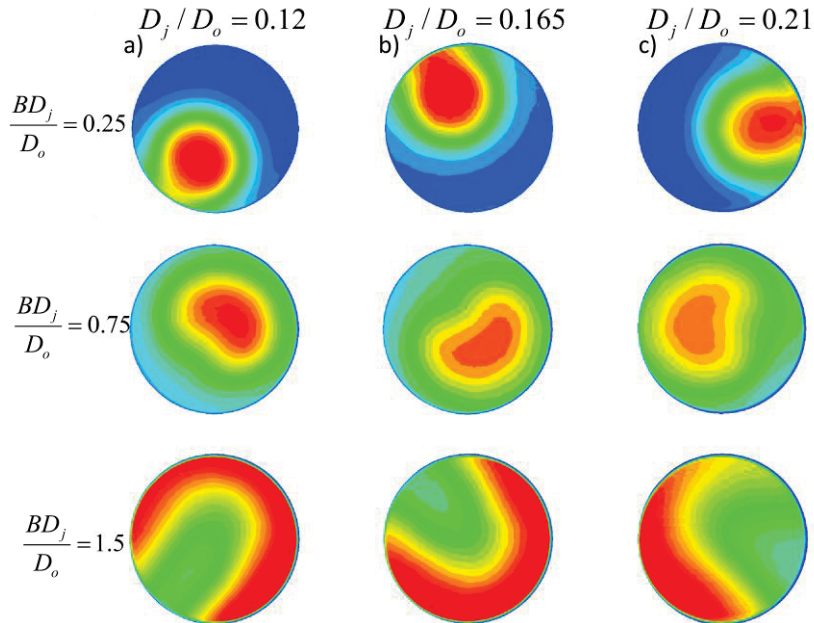


Figure 11: Mean mixture fraction distributions for single transverse jets for diameter ratios of a) 0.12, b) 0.165, and c) 0.21.

to minimal laser absorption for the given experimental length scales.³⁹ The light sheet was located at an $x/D = 3.0$, with the x -axis being located along the centerline of the main pipe with the origin at the centerplane of the injection station.

been shown to satisfy the Holdeman optimum mixing scaling law. Preliminary data has been collected with this experiment using a single confined transverse jet. Figure 10 shows a schematic of the experimental facility. Demineralized water was used for the main and jet fluid, and the jet and main flow were round fully-developed turbulent pipe flow; the Reynolds numbers of the pipe and jet flows are maintained above 6000. The experimental data to be presented will be for one transverse jet; future studies will explore up to six jets issuing into the main flow.

The 488 nm line is isolated from the multiline laser output using an Edmund Optics dichroic mirror. A Phantom V7.1 CMOS camera is used to capture PLIF images; a sample short exposure time image is shown in Fig. 10. A Thorlabs long pass optical filter is placed between the camera and the light sheet to remove the 488 nm from the fluorescence signal. Calibration images were collected for uniform mixtures at different concentration levels. The camera and the fluorescence were independently verified as being nominally linear in the range used for the experiments. The fluorescein concentration in the test section was found to be below approximately 3×10^{-7} mol/L, a level that corresponds

Mean distributions of mixture fraction for some select cases are shown in Fig. 11. The mixture fraction is the local fraction of jet fluid present in the measurement plane and is based on the measured value and the calibration data. Calibration data is pixel specific to account for the Gaussian laser distribution, the spreading of the light sheet, and streaks in the sheet due to imperfections in the test section and/or laser optics.

Figure 11 indicates that constant values of BD_j/D_o for different jet sizes experience similar qualitative distributions. At a BD_j/D_o value of 0.25, the transverse jet has moderate penetration into the main flow (at this measurement location). At a BD_j/D_o of 0.75, the jet has penetrated across the centerline and jet fluid is present across the whole cross section. At a higher BD_j/D_o value of 1.5, the jet has impacted strongly on the wall and spread in the azimuthal direction, resulting in a lower concentration of jet fluid along the center region of the main pipe. The cases for the diameter ratio of 0.21 indicate some asymmetry that will be investigated in the near future. The results indicate that the parameter BD_j/D_o appears to capture the physics, at least to first order, that govern the trajectory of the transverse jet that in turn dictates the regime of penetration/impaction.

The unmixedness of the mixture fraction distribution can be quantified using a variety of definitions. Following the general approach used by Holdeman and coworkers, the unmixedness is defined as

$$U_z = \frac{\sigma}{\sqrt{\bar{Z}(1-\bar{Z})}} \quad (18)$$

where σ is the standard deviation of the mean mixture fraction measurements in the cross plane, and \bar{Z} is the mean mixture fraction based on the relative flow rates and is defined as

$$\bar{Z} = \frac{Q_j}{Q_j + Q_o} \quad (19)$$

The denominator represents the theoretical standard deviation that would be expected if no mixing were occurring and neglects the influence of the velocity field. The actual cross-sectional average of the mean mixture fraction distribution is in general different from \bar{Z} due to the latter being a mass flow weighted quantity while the former is simply an area average. The quantity $(1-U_z)$ can be thought of as an efficiency of mixing for a specific geometry and operating point.

Figure 12 shows the unmixedness parameter U_z as a function of jet to main flow diameter ratio D_j/D_o and flow parameter BD_j/D_o . It is clear that the shape of the unmixedness curves is very similar for all geometries, and the use of the scaling parameter BD_j/D_o provides alignment of the curves, particularly the local optimum point. The figure indicates that the optimum point appears to have the same level of unmixedness at a nominal BD_j/D_o value of 0.75.

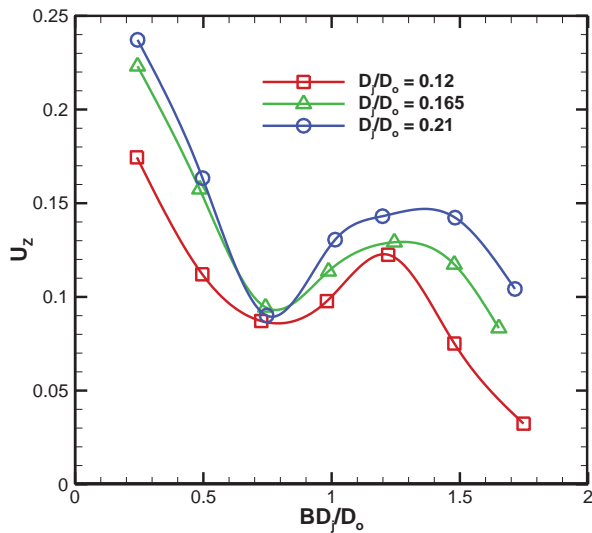


Figure 12: Unmixedness as a function of BD_j/D_o for different relative jet sizes

Recent experimental data collected at AFRL has demonstrated the utility of the new scaling parameter BD_j/D_o to define flow regime and correlate unmixedness. Future research will investigate the use of multiple confined transverse jets and identify scaling parameters for predicting regime and mixing performance.

V. Conclusions

A new scaling law for unconfined transverse jets is proposed that incorporates entrainment and drag effects on the momentum transport to the jet. The new scaling law appears to correlate data in literature on jet trajectory. The new scaling law appears to have application to single and double confined transverse jets (tee mixers). Analysis of entrainment characteristics for configurations with eight or more jets indicate that entrainment is likely to be limited by the available cross flow fluid. A more detailed scaling law format is required to model the effects of confinement on entrainment and drag for eight or more jets.

References

1. Margason, R. "Fifty years of jet in cross flow research," *AGARD Computational and Experimental Assessment of Jets in Cross Flow*. Vol. 1, 1993.
2. Karagozian, A. "Transverse jets and their control," *Progress in Energy and Combustion Science* Vol. 36, No. 5, 2010, pp. 531-553.
3. Fric, T., and Roshko, A. "Vortical structure in the wake of a transverse jet," *Journal of Fluid Mechanics* Vol. 279, 1994, pp. 1-47.
4. Broadwell, J., and Breidenthal, R. "Structure and mixing of a transverse jet in incompressible flow," *Journal of Fluid Mechanics* Vol. 148, 1984, pp. 405-412.
5. Cortelezzi, L., and Karagozian, A. "On the formation of the counter-rotating vortex pair in transverse jets," *Journal of Fluid Mechanics* Vol. 446, 2001, pp. 347-373.
6. Kelso, R., Lim, T., and Perry, A. "An experimental study of round jets in cross-flow," *Journal of Fluid Mechanics* Vol. 306, 1996, pp. 111-144.
7. Sykes, R., Lewellen, W., and Parker, S. "On the vorticity dynamics of a turbulent jet in a crossflow," *Journal of Fluid Mechanics* Vol. 168, 1986, pp. 393-413.
8. Yuan, L., Street, R., and Ferziger, J. "Large-eddy simulations of a round jet in crossflow," *Journal of Fluid Mechanics* Vol. 379, 1999, pp. 71-104.
9. Marzouk, Y., and Ghoniem, A. "Vorticity structure and evolution in a transverse jet," *Journal of Fluid Mechanics* Vol. 575, 2007, pp. 267-305.
10. De B. Alves, L., Kelly, R., and Karagozian, A. "Transverse-jet shear-layer instabilities. Part 2. Linear analysis for large jet-to-crossflow velocity ratio," *Journal of Fluid Mechanics* Vol. 602, 2008, pp. 383-401.
11. Megerian, S., Davitian, J., de B. Alves, L., and Karagozian, A. "Transverse-jet shear-layer instabilities. Part 1. Experimental studies," *Journal of Fluid Mechanics* Vol. 593, 2007, pp. 93-129.
12. Keffer, J., and Baines, W. "The round turbulent jet in a cross-wind," *Journal of Fluid Mechanics* Vol. 15, No. 04, 1963, pp. 481-496.
13. Pratte, B., and Baines, D. "Profiles of the round turbulent jet in a cross flow," *J. Hydronaut. Div. ASCE* Vol. 92, 1967, pp. 53-64.
14. Hasselbrink, E., and Mungal, M. "Transverse jets and jet flames. Part 1. Scaling laws for strong transverse jets," *Journal of Fluid Mechanics* Vol. 443, 2001, pp. 1-25.
15. Ricou, F., and Spalding, D. "Measurements of entrainment by axisymmetrical turbulent jets," *Journal of Fluid Mechanics* Vol. 11, 1961, pp. 21-32.
16. Holdeman, J., Liscinsky, D., and Bain, D. "Mixing of multiple jets with a confined subsonic crossflow: Part II—opposed rows of orifices in rectangular ducts," *Journal of Engineering for Gas Turbines and Power* Vol. 121, 1999, pp. 551-563.
17. Holdeman, J., Srinivasan, R., and Berenfeld, A. "Experiments in dilution jet mixing," *AIAA Journal* Vol. 22, No. 10, 1984, pp. 1436-1443.
18. Holdeman, J., and Walker, R. "An empirical model for the mixing of a row of dilution jets with a confined crossflow," *14th Aerospace Sciences Meeting*. AIAA, Washington, D.C., 1976.
19. Holdeman, J. "Mixing of multiple jets with a confined subsonic crossflow," *Progress in Energy and Combustion Science* Vol. 19, No. 1, 1993, pp. 31-70.
20. Bain, D., Smith, C., and Holdeman, J. "Mixing analysis of axially opposed rows of jets injected into confined crossflow," *Journal of Propulsion and Power* Vol. 11, No. 5, 1995, pp. 885-893.

21. Leong, M., Samuelsen, G., and Holdeman, J. "Optimization of jet mixing into a rich, reacting crossflow," *36th Aerospace Sciences Meeting and Exhibit*. AIAA, Reno, NV, 1998.
22. Leong, M., Samuelsen, G., and Holdeman, J. "Optimization of jet mixing into rich, reacting crossflow," *Journal of Propulsion and Power* Vol. 16, No. 5, 2000, pp. 729-735.
23. Forney, L. "Jet injection for optimum pipeline mixing," *Encyclopedia of Fluid Mechanics* Vol. 2, 1986, pp. 660-690.
24. Maruyama, T., Mizushima, T., and Hayashiguchi, S. "Optimum conditions for jet mixing in turbulent pipe flow," *International Chemical Engineering* Vol. 23, No. 4, 1983, pp. 707-716.
25. Maruyama, T., Mizushima, T., and Watanabe, F. "Turbulent mixing of two fluid streams at an oblique branch," *International Chemical Engineering* Vol. 22, No. 2, 1982, pp. 287-294.
26. Maruyama, T., Suzuki, S., and Mizushima, T. "Pipeline mixing between two fluid streams meeting at a T-junction," *International Chemical Engineering* Vol. 21, No. 2, 1981, pp. 205-212.
27. Pan, G., and Meng, H. "Experimental study of turbulent mixing in a tee mixer using PIV and PLIF," *AIChE Journal* Vol. 47, No. 12, 2001, pp. 2653-2665.
28. O'Leary, C., and Forney, L. "Optimization of in-line mixing at a 90. degree. tee," *Industrial & Engineering Chemistry Process Design and Development* Vol. 24, No. 2, 1985, pp. 332-338.
29. Sroka, L., and Forney, L. "Fluid mixing with a pipeline tee: Theory and experiment," *AIChE Journal* Vol. 35, No. 3, 1989, pp. 406-414.
30. Cozewith, C., and Busko Jr, M. "Design correlations for mixing tees," *Industrial & Engineering Chemistry Research* Vol. 28, No. 10, 1989, pp. 1521-1530.
31. Forney, L., Nafia, N., and Vo, H. "Optimum jet mixing in a tubular reactor," *AIChE Journal* Vol. 42, No. 11, 1996, pp. 3113-3122.
32. Muppidi, S., and Mahesh, K. "Study of trajectories of jets in crossflow using direct numerical simulations," *Journal of Fluid Mechanics* Vol. 530, 2005, pp. 81-100.
33. Gutmark, E., Ibrahim, I., and Murugappan, S. "Circular and noncircular subsonic jets in cross flow," *Physics of Fluids* Vol. 20, No. 7, 2008, pp. 5110-5126.
34. Mashayek, A., Jafari, A., and Ashgriz, N. "Improved model for the penetration of liquid jets in subsonic crossflows," *AIAA Journal* Vol. 46, No. 11, 2008, pp. 2674-2686.
35. Han, D., and Mungal, M. "Direct measurement of entrainment in reacting/nonreacting turbulent jets," *Combustion and flame* Vol. 124, No. 3, 2001, pp. 370-386.
36. New, T., Lim, T., and Luo, S. "Effects of jet velocity profiles on a round jet in cross-flow," *Experiments in Fluids* Vol. 40, No. 6, 2006, pp. 859-875.
37. Smith, S., and Mungal, M. "Mixing, structure and scaling of the jet in crossflow," *Journal of Fluid Mechanics* Vol. 357, 1998, pp. 83-122.
38. Han, D., Mungal, M., and Orozco, V. "Gross-entrainment behavior of turbulent jets injected obliquely into a uniform crossflow," *AIAA Journal* Vol. 38, No. 9, 2000, pp. 1643-1649.
39. Walker, D. "A fluorescence technique for measurement of concentration in mixing liquids," *Journal of Physics E: Scientific Instruments* Vol. 20, 1987, p. 217.